

Synthesis and X-ray investigation of new $Y_{1-x}R_xCa_4O(BO_3)_3$ ($R = Sc, Lu$) nonlinear materials

L. GHEORGHE^{*}, A. ACHIM, B. SBARCEA^a, S. MITREA^a

National Institute R&D for Laser, Plasma and Radiation Physics, Laboratory of Solid-State Quantum Electronics, 077125, Bucharest-Magurele, Romania

^aNational Institute R&D in Electrical Engineering ICPE-CA, Laboratory for materials and electrotechnical products testing and characterizations, 030138, Bucharest, Romania

Nonlinear materials $Y_{1-x}R_xCa_4O(BO_3)_3$ ($R = Lu$ or Sc) with $0 < x \leq 0.5$ were synthesized for the first time. The room temperature X-ray diffraction studies show that $Y_{1-x}Lu_xCa_4O(BO_3)_3$ and $Y_{1-x}Sc_xCa_4O(BO_3)_3$ compounds with $x < 0.4$ and $x \leq 0.2$, respectively, have single phase monoclinic symmetry (space group Cm) and conform to the Vegard law, according to which the lattice parameters are linearly dependent on the impurity (R^{3+}) concentration. The X-ray patterns of $Y_{1-x}R_xCa_4O(BO_3)_3$ materials with $x \geq 0.4$ and $x > 0.2$, respectively, reveal the presence of extra phases which imply their non-congruent melting and difficulties in crystals growth.

(Received February 25, 2010; accepted March 12, 2010)

Keywords: Nonlinear materials, Solid solutions, Rare earth calcium oxoborates, X-ray powder diffraction

1. Introduction

In recent years, there has been a growing demand for specific visible and ultraviolet laser sources in medicine, industrial processing, remote sensing, laser printing, optical displays, and other areas. At this time, the availability of laser frequencies in the visible-UV range is limited by laser materials and pump sources. Frequency conversion of solid-state lasers operating in the near infrared range by nonlinear optical (NLO) crystals has become the most available method to obtain shorter wavelength lasers with high beam stability, low cost and compactness. Thus, the reliance on nonlinear methods of frequency generation demonstrates the need for new nonlinear harmonic crystals with the ability to frequency convert a wide variety of laser wavelengths. The current approach to achieve visible-UV efficient laser radiation is by second-harmonic generation (SHG) in NLO crystals of diode-pumped solid state laser infrared emission, in noncritical phase-matching (NCPM) conditions. For frequency conversion applications, the NCPM is advantageous because of its large angular acceptance and because it eliminates walk-off between fundamental and harmonic radiations which leads to the highest efficiency.

Rare earth calcium oxoborate crystals $ReCa_4O(BO_3)_3$ - $ReCOB$ ($Re = La^{3+}, Gd^{3+}, Y^{3+}$) are congruent melting nonlinear materials allowing the growth of large dimension crystals to be used as frequency converter in solid state laser systems [1 - 5]. $YCa_4O(BO_3)_3$ (YCOB) crystal combines some of the more attractive mechanical and optical properties in one crystal in comparison with the most commonly used NLO crystals (KDP, KTP, BBO, and LBO) [3, 6]. Previously, it was found that the substitution of the trivalent Re cations with smaller radius cations lead to larger optical birefringence [7, 8]. In

YCOB crystal, the Y^{3+} ions can be partially substituted by smaller radius ions Sc^{3+} or Lu^{3+} in order to tune the chemical composition of the crystal. By changing the compositional parameter x of $Y_{1-x}R_xCa_4O(BO_3)_3$ ($R = Lu, Sc$) crystals, their optical birefringence can be controlled in order to achieve NCPM SHG of specific near infrared laser emission wavelengths shorter than phase-matching cutoff wavelength of YCOB crystal (724 nm along Y axis and 832 nm along Z axis at room temperature [9]). According to the ionic radii of R^{3+} ions ($r_{Lu} = 0.861 \text{ \AA}$, $r_{Sc} = 0.745 \text{ \AA}$, $r_Y = 0.9 \text{ \AA}$ [10]), the effect on magnitude of optical birefringence is more stronger in case of substitution with Sc^{3+} ions and the optical birefringence increases with increasing of compositional parameter x .

$ScCa_4O(BO_3)_3$ and $LuCa_4O(BO_3)_3$ compounds do not have congruent melting and single crystals with these compositions cannot be grown from the melt. Ilyukhin and Dzhurinskii [11] made structural investigations of $LuCa_4O(BO_3)_3$ tiny crystals, grown from a PbO flux. Consequently, in YCOB structure the Sc^{3+} or Lu^{3+} ions can only partially substitute Y^{3+} ions depending on their ion sizes. Therefore, the main problem is to establish the solubility limit of Sc^{3+} and Lu^{3+} ions. In this aim, synthesis of $Y_{1-x}R_xCa_4O(BO_3)_3$ nonlinear materials, experimental establishment of the solubility region of R^{3+} ions in YCOB structure and X-ray diffraction study of $Y_{1-x}R_xCa_4O(BO_3)_3$ solid solutions are reported in this work.

2. Experimental

2.1 Sample preparation

$Y_{1-x}Lu_xCa_4O(BO_3)_3$ and $Y_{1-x}Sc_xCa_4O(BO_3)_3$ compounds with $x = 0.0, 0.1, 0.2, 0.3, 0.4$ and 0.5 were

prepared by solid state reaction. Chemicals of Y_2O_3 , $CaCO_3$, B_2O_3 , Lu_2O_3 , and Sc_2O_3 of 99.99% purity were used as starting materials. In order to eliminate the absorbed water, the $CaCO_3$ powder was preheated at $400^\circ C$ for 10 h. According with the following reaction:



the compounds were immediately weighed in stoichiometric ratio and mixed by milling in an agate mortar until fine powders were obtained. Then they were cold-pressed into cylindrical pellets and heated at $900^\circ C$ for 15h to decompose $CaCO_3$ completely. Subsequently, the obtained pellets were crushed, mixed and pressed again into pellets and annealed for $1350^\circ C$ for 24h.

2.2 X-ray powder diffraction

The X-ray powder diffraction (XRPD) patterns of the $Y_{1-x}R_xCa_4O(BO_3)_3$ synthesised samples were recorded with a Bruker AXS D8 ADVANCE X-ray diffractometer ($Cu K_{\alpha 1} = 1.5406 \text{ \AA}$). The measurements were carried out at room temperature between 10° and 70° in 2θ using a flat rotating sample holder. The angular resolution of the apparatus was better than 0.014° . The XRPD data were analyzed with the Rietveld profile refinement method [12] using TOPAS V2.1 software [13]. The Rietveld method employs total pattern fitting between the observed and calculated intensity for every data point in the diffraction pattern. The continuous background, the unit cell parameters, the displacement of the surface sample with regard to the focusing circle and the profile of the diffraction peaks were refined for each sample.

3. Results and discussion

$ReCa_4O(BO_3)_3$ ($Re = La^{3+}, Gd^{3+}, Y^{3+}$) compounds have a non centro-symmetric monoclinic structure, with space group Cm [1, 11]. Their structure contains a Re site of Cs symmetry, two types of calcium sites $Ca^{2+}(1)$ and $Ca^{2+}(2)$ and two distinct $(BO_3)^{3-}$ groups. In the case of $YCa_4O(BO_3)_3$ the unit cell parameters are $a = 8.077 \text{ \AA}$, $b = 16.019 \text{ \AA}$, $c = 3.530 \text{ \AA}$ and $\beta = 101.167^\circ$ [14]. Six close oxygen, two B^{3+} ions and two O^{2-} at larger distances than borons coordinate the Re^{3+} ion. Two nearest oxygen ions to the Re^{3+} cation, labeled O(1), do not belong to the borate groups, while the other six oxygen ions are members of these groups. Ca^{2+} occupy two sites of C_1 symmetry, $Ca^{2+}(1)$ in a sixfold O^{2-} coordination and $Ca^{2+}(2)$ in a distorted eightfold O^{2-} coordination and with two B^{3+} ions intercalated between the first six O^{2-} and the other two.

The room temperature XRD patterns of $Y_{1-x}Lu_xCa_4O(BO_3)_3$ and $Y_{1-x}Sc_xCa_4O(BO_3)_3$ samples with different compositional parameter x are presented in Figs. 1 and 2, respectively. As we can observe all synthesized $Y_{1-x}R_xCa_4O(BO_3)_3$ compounds are, or contain a major phase, isostructural with monoclinic YCOB ($x = 0$). Thus $Y_{1-x}Lu_xCa_4O(BO_3)_3$ and $Y_{1-x}Sc_xCa_4O(BO_3)_3$ compounds with $x < 0.4$ and $x \leq 0.2$, respectively, have single phase monoclinic symmetry, $Y_{1-x}Lu_xCa_4O(BO_3)_3$ compounds with $x \geq 0.4$ contain two minor extra phases Y_2O_3 [15] and CaO [16] while $Y_{1-x}Sc_xCa_4O(BO_3)_3$ compounds with $x > 0.2$ contain also two minor parasitic phases $Ca_3B_2O_6$ [17] and CaO . It can be noticed from both figures that peaks shift towards higher angle indicating decrease of the lattice parameters for the single phase and monoclinic major phase compositions. Concerning the growth of large $Y_{1-x}R_xCa_4O(BO_3)_3$ crystals from melt, it is also very important to note that according to obtained results the melting of $Y_{1-x}Lu_xCa_4O(BO_3)_3$ and $Y_{1-x}Sc_xCa_4O(BO_3)_3$ solid solutions with $x \geq 0.4$ and $x > 0.2$, respectively, is no longer congruent which imply difficulties in their growing.

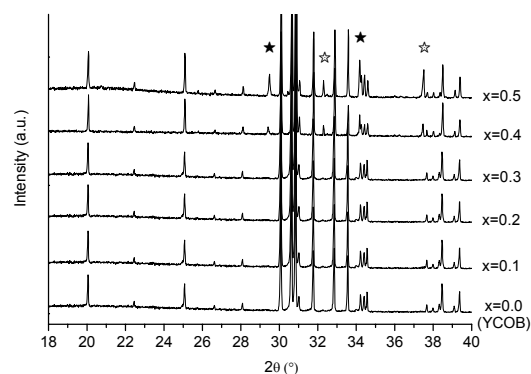
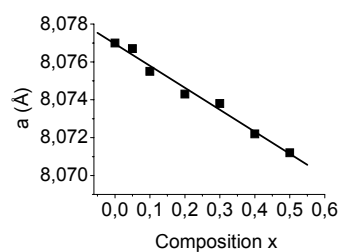
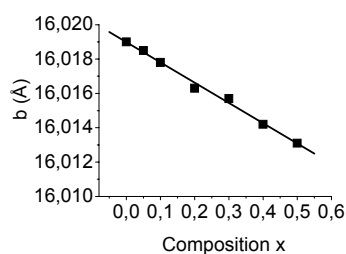


Fig. 1. Room temperature XRD patterns of $Y_{1-x}Lu_xCa_4O(BO_3)_3$ samples with different compositional parameter x . The peaks marked with full and open stars belong to Y_2O_3 [15] and CaO [16] parasitic phases, respectively.

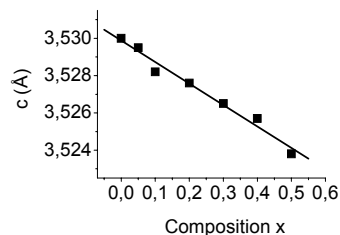
The structure refinements for the single phase compounds and the major monoclinic phase in the case of polyphasic compounds, were initiated using the reported space group (Cm) and the atomic coordinates for $YCa_4O(BO_3)_3$ [14] with the substitutional R atoms incorporated into the Y atomic sites. The lattice parameters of both type synthesized materials ($Y_{1-x}Lu_xCOB$ and $Y_{1-x}Sc_xCOB$) as function of compositional parameter x are plotted in figures 3(a, b, c, d and e) and 4(a, b, c, d and e), respectively.



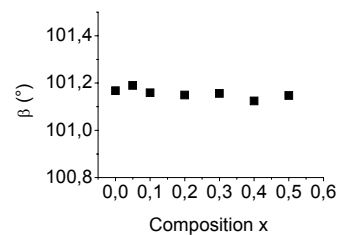
(a)



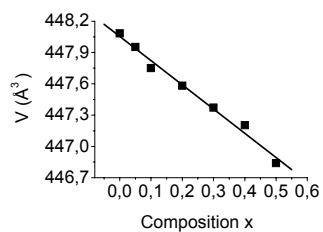
(b)



(c)

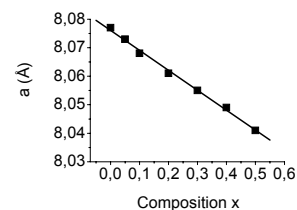


(d)

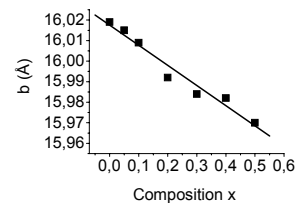


(e)

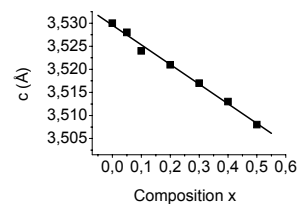
Fig. 3. Unit cell parameters of $Y_{1-x}Lu_xCa_4O(BO_3)_3$ solid solutions as function of composition. The error bars are smaller than the symbols.



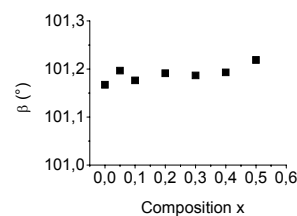
(a)



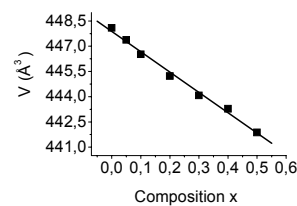
(b)



(c)



(d)



(e)

Fig. 4. Unit cell parameters of $Y_{1-x}Sc_xCa_4O(BO_3)_3$ solid solutions as function of composition. The error bars are smaller than the symbols.

According to the Vegard's law [18], the lattice parameters a , b and c linearly decrease with the increasing of the substitution degree of Y^{3+} ions with R^{3+} ions. Corresponding to the ionic radii of R^{3+} ions, the decreasing

is stronger in the case of substitution with smaller Sc^{3+} ions. The angle β remains practically constant. The unit cell volume of the monoclinic phase decreases also linearly with increasing of x . According to the ionic radii of R^{3+} ions, the effect is more important for $Y_{1-x}Sc_xCa_4O(BO_3)_3$ solid solutions.

4. Conclusions

New nonlinear materials $Y_{1-x}R_xCa_4O(BO_3)_3$ (with $x = 0.0, 0.1, 0.2, 0.3, 0.4$ and 0.5) have been synthesized by solid state reaction method. The room temperature XRPD studies show that for $Y_{1-x}Lu_xCa_4O(BO_3)_3$ compounds the solubility limit of Lu^{3+} ions in YCOB is $< 40\%$ ($x < 0.4$) and for $Y_{1-x}Sc_xCa_4O(BO_3)_3$ compounds the solubility limit of Sc^{3+} ions in YCOB is $\leq 20\%$ ($x \leq 0.2$). Over these doping limits $Y_{1-x}R_xCa_4O(BO_3)_3$ materials have a non-congruent melting leading to the formation of less two parasitic phase (Y_2O_3 and CaO for $Y_{1-x}Lu_xCOB$ compositions and $Ca_3B_2O_6$ and CaO in the case of $Y_{1-x}Sc_xCOB$ compounds) which make more difficult their growth from melt which large dimensions. $Y_{1-x}R_xCa_4O(BO_3)_3$ crystal growth experiments with compositional parameter x inside the established solubility domains are now in progress.

Acknowledgements

This work was supported by the "Partnerships" Romanian Research Programme of the National Plan II (NP II), Contract No. 12105/2008.

References

- [1] R. Norrestam, M. Nygren, J. O. Bovin, *Chem. Mater.* **4**, 738 (1992).
- [2] G. Aka, A. Kahn-Harari, D. Vivien, J.-M. Benitez, F. Salin, J. Godard, *Eur. J. Solid State Inorg. Chem.* **33**, 727 (1996).
- [3] M. Iwai, T. Kobayashi, H. Furuya, Y. Mori, T. Sasaki, *Jpn. J. Appl. Phys.* **36**, L276 (1997).
- [4] J. J. Adams, C. A. Ebbers, K. I. Schaffers, S. A. Payne, *Opt. Lett.* **26**, 217 (2001).
- [5] D. Klimm, S. Ganschow, R. Bertram, J. Doerschel, V. Bermudez, A. Klos, *Mater. Res. Bull.* **37**(10), 1737 (2002).
- [6] S. Zhang, Z. Cheng, Y. Sun, J. Liu, Z. Wang, J. Lv, X. Hou, J. Wang, Z. Shao, H. Chen, *Phys. Stat. Sol. (a)* **183**(2), 435 (2001).
- [7] H. Furuya, M. Yoshimura, T. Kobayashi, K. Murase, T. Sasaki, *J. Cryst. Growth*, **198/199**, 560 (1999).
- [8] H. Nakao, S. Makio, H. Furuya, K. Kawamura, S. Yasuda, Y. K. Yap, M. Yoshimura, Y. Mori, T. Sasaki, *J. Cryst. Growth* **237-239**, 632 (2002).
- [9] N. Uemura, K. Yoshida, H. Nakao, H. Furuya, M. Yoshimura, Y. Mori, T. Sasaki, K. Kato, *Jpn. J. Appl. Phys.* **40**, 596 (2001).
- [10] R. D. Shanon, *Acta Crystallogr.* **32A**, 751 (1976).
- [11] B. Ilyukhin, B. F. Dzhurinskii, *Russian J. Inorg. Chem.* **38**, 847 (1993).
- [12] R. A. Young (Ed.), *The Rietveld Method*, Oxford University Press, Oxford, 1993.
- [13] Bruker Advanced X-ray Solutions TOPAS V2.0, User Manual, Bruker AXS, Version 2, Karlsruhe, Germany, 2000.
- [14] F. Mougél, Thèse de doctorat de l'Université Paris VI (1999) (pastel.paristech.org/1068/01/mougel.pdf).
- [15] JCPDS-International Center for Diffraction Data, Standard JCPDS diffraction pattern, Reference code 00-043-0661, PDF index name: Yttrium Oxide.
- [16] JCPDS-International Center for Diffraction Data, Standard JCPDS diffraction pattern, Reference code 01-077-2010, PDF index name: Calcium Oxide.
- [17] JCPDS-International Center for Diffraction Data, Standard JCPDS diffraction pattern, Reference code 00-048-1855, PDF index name: Calcium Borate.
- [18] L. Vegard, Die Konstitution der Mischkristalle und die Raumfüllung der Atome, *Zeitschrift für Physik* **5**, 17 (1921).

*Corresponding author: lucian.gheorghe@inflpr.ro